J Vis (2016) 19:1–5
DOI 10.1007/s12650-015-0303-0

SHORT PAPER

K. Peter Judd · Ivan Savelyev · Qi Zhang · Robert A. Handler

The thermal signature of a submerged jet impacting normal to a free surface

Received: 12 December 2014 / Revised: 26 March 2015 / Accepted: 19 May 2015 / Published online: 4 July 2015

1 Introduction

In recent years, infrared (IR) sensors with high thermal, spatial, and temporal resolution have been used to explore the dynamics and structure of fluid flows. Much of this work has focused on understanding complex flows at an air–water interface. Laboratory-scale phenomena at such interfaces have been explored using IR methods by Handler et al. (2001), Smith et al. (2001), Phongikaroon et al. (2004), Judd et al. (2005), Phongikaroon and Judd (2006), Scott et al. (2008), Judd et al. (2008), Handler and Smith (2011), and Voropayev et al. (2014). Geophysical-scale processes have also been explored recently using these methods by Jessup et al. (1997), Marmorino et al. (2004), Marmorino and Smith (2005), and Marmorino et al. (2005). Other recent studies have examined the impingement of jets onto free surfaces (Larocque et al. 2009) and solid boundaries (Hadziabdic and Hanjalic 2008). Aside from the IR sensor characteristics, the properties of water make such explorations possible. In particular, since the Prandtl number of water at ordinary temperatures is about 7, heat becomes an excellent tracer of fluid motions. In addition, the optical depth of radiation at infrared wavelengths is on the order of tens of microns. For example, the IR sensor in this study detects radiation in the 3–5 μm waveband for which the optical depth in water is about 35 μm. For this reason, only surface temperatures can be obtained in this wavelength range. Judd et al. (2008) used IR methods to investigate the flow of a turbulent jet whose mean flow was parallel to a free surface. In that investigation, certain features of the flow were revealed such as a surface current first observed by Anthony and Willmarth (1992), the migration of the centerline mean peak temperature upstream with increasing Reynolds number suggesting a tendency toward greater instability, and a departure from a single temperature field scaling suggesting the existence of inner and outer regions in the jet flow. Here we explore the case where the mean flow of a turbulent jet impinges normal to the free surface. Such flows are of interest in the study of mixing of discharge flow from large scale outflows from power plants and the surrounding receiving water mass [Marmorino et al. (2014)].

Electronic supplementary material The online version of this article (doi:10.1007/s12650-015-0303-0) contains supplementary material, which is available to authorized users.

K. P. Judd (✉) · I. Savelyev
Naval Research Laboratory, Washington, DC 20375, USA
E-mail: kjudd@ccs.nrl.navy.mil; kyle.judd@nrl.navy.mil
Tel.: +2024047494

Q. Zhang · R. A. Handler
Department of Mechanical Engineering, Texas A&M University, College Station, TX, USA

2 Experimental methods

A turbulent round jet was formed by forcing water through a nozzle of exit diameter $D = 0.635$ cm. The jet, whose axis was perpendicular to an air–water interface, was formed in a large water basin 22 cm beneath the interface. To reduce the influence of the basin side walls, the jet was placed equidistant from the walls. The temperature excess between the water used to form the jet and that of the water basin was ~ 3 °C. In Fig. 1, a laser-induced fluorescence image of a turbulent jet is shown for a Reynolds number, $Re = U_J D/\nu = 4800$, where U_J is the average velocity of the jet, and ν is the kinematic viscosity of water. It is evident from the figure that beyond a short transition distance of a few centimeters, the jet appears fully turbulent. Thermal imagery was obtained using a FLIR systems SC6000 research grade mid-wave infrared camera with a sensing array of size 640 $\times$ 512 pixels, a dynamic range of 14 bits, and a thermal sensitivity of ~ 18 mK. The camera was mounted looking down on the free surface with a line of sight directly perpendicular to the surface. All IR images shown here, which were obtained while the camera was in this configuration, can then be interpreted as temperature maps of the water surface during the period of time in which jet–free surface interaction was taking place.

3 Results

Infrared imagery of the free surface was obtained during the period in which the jet was fully turbulent. At each of two Reynolds numbers, $Re = 1720$ and 4800, 2000 images were obtained at a frame rate of 60 Hz, which translates into a time period of 33.33 s. These images (frames) represent instantaneous snapshots of the surface temperature field. From these snapshots any desirable statistic of the thermal field can be obtained such as the mean temperature, $\overline{\theta}$, and the root mean square (rms) temperature, θ_{rms} defined by:

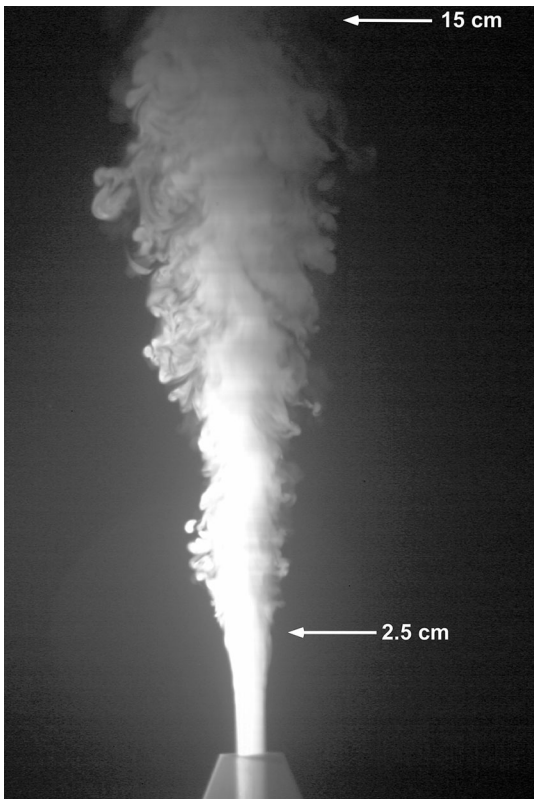

Fig. 1 Laser-induced fluorescence image of the turbulent water jet with $Re = 4800$ directed normal to a free surface. Here the jet can be seen exiting an orifice ~ 22 cm beneath the free surface. A transition region, in which the jet undergoes transition to a fully developed turbulent flow, is evident in a region ~ 2.5 cm above the end of the nozzle

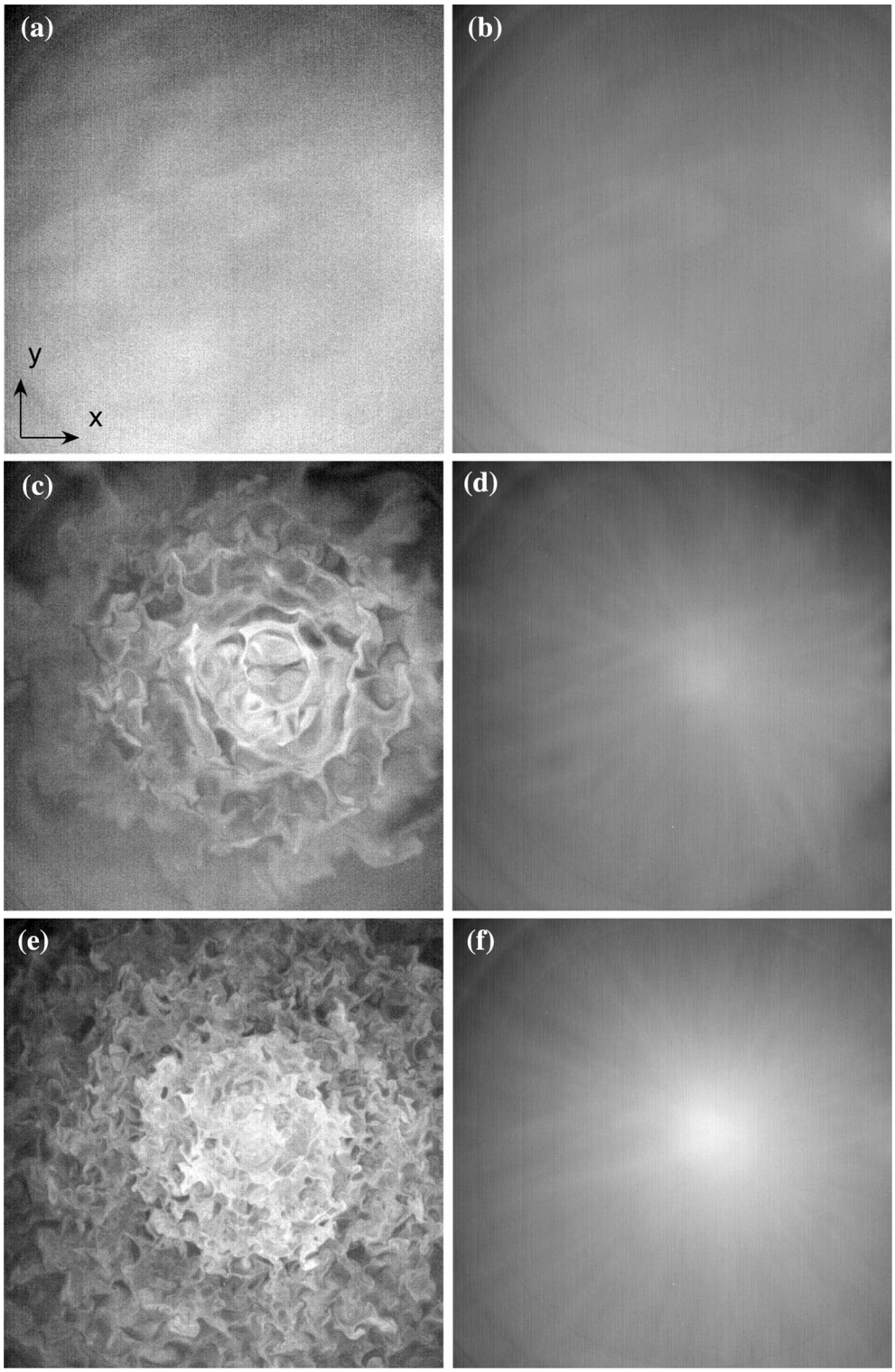

Fig. 2 Infrared imagery of the impact zone where the turbulent jet impinges onto the free surface for $Re = 0$ no flow (**a**, **b**), $Re = 1720$ (**c**, **d**), and $Re = 4800$ (**e**, **f**). Each image is 50 cm in the horizontal (x) direction and 55 cm in the vertical (y) direction. Instantaneous snapshots of the flow are in the *left column* and the mean fields are in the *right column*

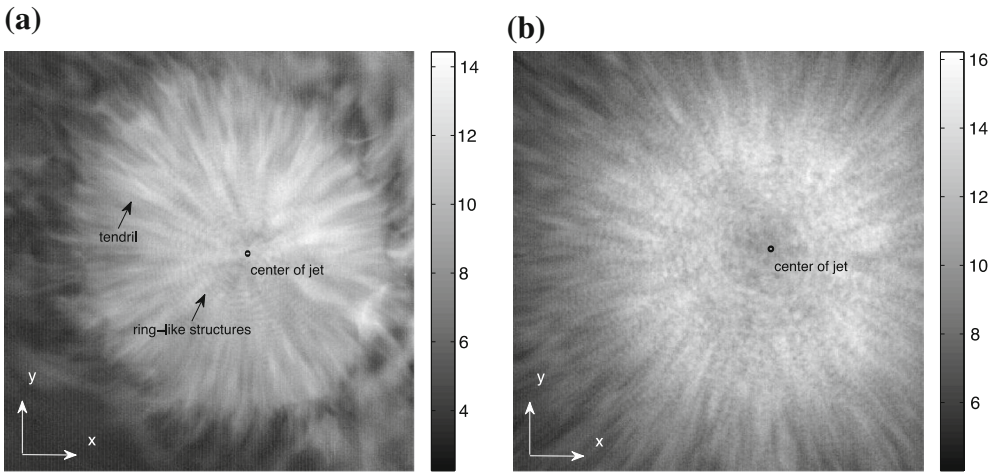

Fig. 3 Root mean square temperature fluctuations for $Re = 1720$ (**a**) and $Re = 4800$ (**b**). Units of the *grayscale bars* are in 'counts' where one count represents ~ 0.018 °C. The images have the same physical dimensions as those in Fig. 2

$$\bar{\theta}(x,y) = \frac{1}{N}\sum_{n} \theta_n(x,y), \tag{1a}$$

and

$$\theta_{\mathrm{rms}}(x,y) = \left[\frac{1}{N}\sum_{n} [\theta_n(x,y) - \bar{\theta}(x,y)]^2\right]^{1/2} \tag{1b}$$

where $\theta_n(x,y)$ is the temperature field on the free surface at the spatial point (x, y), n is the index corresponding to the frame number, and N is the total number of frames.

The images in the left-hand column of Fig. 2 are instantaneous temperature fields of the flow for a "no flow" condition $Re = 0$, $Re = 1720$, and $Re = 4800$. It is noteworthy that the thermal patterns become more fine grained as the Reynolds number is increased which is consistent with standard Kolmogorov scaling theory (Tennekes and Lumley 1972). The image sequence in the right-hand column is of the mean temperature field, $\overline{\theta}$. In Fig. 3, maps of θ_{rms} for two Reynolds numbers are shown. We note that no flow symmetries (see Judd et al. 2008) were imposed in the creation of these images, so that the expressions above [Eqs. (1a, 1b)] were used literally as stated. A significant feature seen in the images for θ_{rms}, and to a lesser extent in the images of $\overline{\theta}$, are streaks or tendrils associated with regions of large thermal fluctuations which are observed to emanate from the center of the jet impingement region. These tendrils, while evident at each Reynolds numbers, are most prominent at $Re = 1720$. This result was not expected since, given an averaging time of more than half a minute, we might expect that any such coherent features would be smoothed out due to the inherent random nature of turbulence, and the circumferential symmetry of the flow. The existence of these streaky tendrils apparently indicates the existence of a persistent structure associated with the jet flow. At the present time, however, we do not wish to speculate on any particular fluid mechanical or thermal mechanism that may be responsible for the tendrils. Finally we note also that in all cases the turbulence was of sufficient strength that radially propagating gravity–capillary waves were always observed at the free surface. It is interesting to note in these images that faint ring-like structures reminiscent of such waves are evident, though it is not clear whether these structures are in any way related to the observed gravity–capillary waves. Determining the physical origins of the radially oriented tendrils and these ring-like structures will be the subject of future work.

Acknowledgments The first two authors would like to acknowledge the support of the Naval Research Laboratory.

References

Anthony DG, Willmarth WW (1992) Turbulence measurements in a round jet beneath a free surface. J Fluid Mech 243:699–720

Hadziabdic M, Hanjalic K (2008) Vortical structures and heat transfer in a round impinging jet. J Fluid Mech 596:221–260

Handler RA, Smith GB (2011) Statistics of the temperature and its derivatives at the surface of a wind-driven air-water interface. J Geophys Res 116:C06021

Handler RA, Smith GB, Leighton RI (2001) The thermal structure of an air-water interface at low wind speeds. Tellus Ser A 53:233–244

Jessup AT, Zappa CJ, Loewen MR, Hesany V (1997) Infrared remote sensing of breaking waves. Nature 385:52–55

Judd KP, Phongikaroon S, Smith GB, Handler RA (2005) Thermal structure of clean and contaminated free-surfaces subject to an impinging gas jet. Exp Fluids 38:99–111

Judd KP, Smith GB, Handler RA, Sisodia A (2008) The thermal signature of a low Reynolds number submerged turbulent jet impacting a free surface. Phys Fluids 20:115102

Larocque J, Riviere N, Vincent S, Reungoat D, Faure J-P, Heliot J-P, Caltagirone J-P, Moreau M (2009) Macroscopic analysis of a turbulent round liquid jet impinging on an air/water interface in a confined medium. Phys Fluids 21:065110

Marmorino GO, Smith GB (2005) Bright and dark ocean whitecaps observed in the infrared. Geophys Res Lett 32:L11604

Marmorino GO, Smith GB, Lindemann GJ (2004) Infrared imagery of ocean internal waves. Geophys Res Lett 31:L11309

Marmorino GO, Smith GB, Lindemann GJ (2005) Infrared imagery of large-aspect-ratio Langmuir circulation. Cont Shelf Res 25(1):1–6

Marmorino GO, Savelyev I, Smith GB (2014) Surface thermal structure in a shallow-water, vertical discharge from a coastal power plant. Environ Fluid Mech 15(1):207–229

Phongikaroon S, Judd KP (2006) Surfactant effects on the free surface thermal structure and subsurface flow in a wind-wave tunnel. J Fluids Eng 128:913–917

Phongikaroon S, Judd KP, Smith GB, Handler RA (2004) The thermal structure of a wind-driven Reynolds ridge. Exp Fluids 37:153–158

Scott NV, Handler RA, Smith GB (2008) Wavelet analysis of the surface temperature field at an air-water interface subject to moderate wind stress. Int J Heat Fluid Flow 29:1103–1112

Smith GB, Volino RJ, Handler RA, Leighton RI (2001) The thermal signature of a vortex pair impacting a free surface. J Fluid Mech 444:49–78

Tennekes H, Lumley JL (1972) A first course in turbulence. MIT Press, Cambridge

Voropayev SI, Nath C, Fernando HJS (2014) Surface signatures of submerged heated jet. Environ Fluid Mech 14:1105–1121